International Journal of Applied Engineering Research ISSN 0973-4562 Volume 12, Number 17 (2017) pp. 6720-6729

Application of Optimal Pole Shifting Control to Isolated Wind Energy System

I. E. Atawi

Electrical Engineering Department, University of Tabuk, Tabuk 71491, Saudi Arabia.

Orcid: 0000-0001-6816-0885 & Scopus Author ID: 56576396100

Abstract

This article investigates the application of the optimal pole-shifting (OPS) control algorithm to regulate both the voltage and frequency of a load supplied by an autonomous wind power system. This proposed wind energy conversion power system is mainly consists of an induction generator driven by wind turbine and feeds a stand-alone load. The generator terminal voltage is regulated by adjusting the TCR firing angle of the SVC, which is connected at the IG terminals. A wind-blade pitch-angle control is applied to adjust the IG mechanical input power which leading to IG rotor speed, and consequently the load frequency are controlled. A controller design based on OPS approach is applied on the two control loops of SVC and wind-blade pitch control.

Digital simulation results are obtained to validate the effectiveness of the proposed wind-energy control system. In addition, this proposed system has been tested via turbulent changes in the wind speed and step changes in the load impedance. Moreover, a comparison between the proposed optimal pole-shifting controller and LQR is presented. The obtained simulation results show that adequate performance of the studied system has been achieved. The robustness of the proposed controller against parameters variations and modeling errors are tested to proof the superiority of the proposed OPS controller compared with LQR approach.

Keywords: Optimal pole shifting control; wind turbine; induction generator; LQR control; SVC.

INTRODUCTION

Remote area power-generation systems are now becoming popular in remote areas including islands. However, the design and operation of such systems are challenging due to the absence of the main grid supply. In addition, networks having low X/R ratios, low damping, and lack of reactive power control, which may cause unexpected voltage and frequency excursions outside their desired limits [1], usually characterize these power generation systems. In designing and implementing isolated power generation systems, voltage and frequency regulation are the most important aspects to be regulated.

Many electrical generators can be used to implement the Wind Energy Conversion WEC systems, each of which has different advantages and disadvantages [2]–[4]. We saw that the induction generator is generally simpler, cheaper, more reliable, and perhaps more efficient than some other generators. The induction generator and the PM generator are similar in construction, except for the rotor, so complexity, reliability, and efficiency should be quite similar for these two types of machines. However, the induction generator is likely to be cheaper than the PM generator by perhaps a factor of two. Induction motors are used very widely, and it may be expected that many will be used as induction generators because of such factors as good availability, reliability, and reasonable cost [5].

The induction-generator-based wind turbines are considered consumer of reactive power [6]-[16]. To minimize the power losses and increase voltage stability, the reactive power of these wind turbines are compensated. For wind turbines with PWM converter systems, the converter can control the reactive power. Thus, these wind turbines have the possibility to control voltage by controlling the generation or consumption of reactive power. The reactive power control can be conducted by following the load requirement to contribute to the system voltage control; it can also be performed to minimize the possible voltage fluctuations caused by wind power fluctuations. Voltage stability problems may be derived from the need for reactive power of some wind turbines. This fact becomes more import during a voltage dip since in this case; the problem is to generate enough reactive power for the wind generators. One solution for transient and steady state of the load voltage control are the SVC.

Over the past few years, there has been significant research effort in the analysis, modeling, and control design for WT with parametric uncertainties [17]-[21]. Optimal pole shifting control is an effective technique to design control systems. Recently the pole-shift control scheme has been applied in power system applications (Power system stabilizer) and hydro plant system [22]-[25]. However, optimal pole shifting control has not been applied to WEC systems.

In This paper, an optimal pole-shifting controller of autonomous WT system with isolated load are present. The system construction parts, modelling, and optimal pole-shifting controller design are discussed in details. Then, proposed system with the proposed controller has been tested through a step changes in both wind speed and load impedance. A comparison between the proposed optimal pole-shifting controller and LQR is presented. The obtained simulation results show that adequate performance of the studied system has been achieved. Moreover, this proposed controller is robust against the parameters variation and can eliminates the effects of modeling errors and the superiority of the proposed OPS controller compared with LQR approach.

SYSTEM MODELLING

Figure (1) shows the proposed isolated wind power system, which consists of wind turbine drives self-excited induction generator and supplying load via static VAR compensator. For voltage control, a fixed-capacitor thyristor-controlled reactor (TCR) static VAR compensator type is used, which is connected at the IG terminals. In this case, the load voltage is mainly depends on the SVC capacitance, IG rotor speed and the load impedance. While, the frequency of the load voltage is mainly depends on the rotor speed of the induction generator only. Therefore, if the speed of the wind varies and/or if the impedance of the load on the terminals of IG varies, the load voltage and frequency will vary too. Where, this is remonstrance to sensitive loads. In this study, the optimal pole-shifting controller has been applied to overrun this problem.

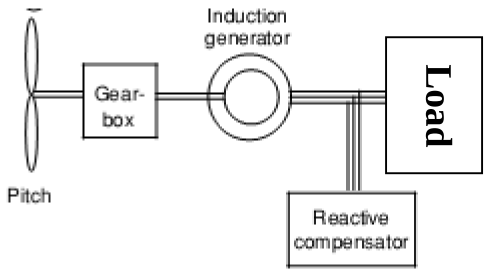

Figure 1: Schematic representation of the wind energy system

Wind Turbine Model

The wind turbine is characterized by no dimensional curves of the power coefficient C_p as a function of both the tip speed ratio λ and the blade pitch angle β. In order to fully utilize the available wind energy, the value of λ should be maintained at its optimum value. Hence, the power coefficient corresponding to that value will be optimum also.

The tip speed ratio λ can be defined as the ratio of the angular rotor speed of the WT to the linear wind speed at the tip of the blades. It can be expressed as follows [26]:

$$\lambda = \omega_t R / V_w \tag{1}$$

Where R is WT rotor radius, V_w is the wind speed and ω_t is the mechanical angular rotor speed of the WT.

The turbine output power P_t, which is a function of the blade angle, the rotor speed, and the wind speed, can be expressed as [26]:

$$P_t = \frac{1}{2}\rho A C_p(\lambda,\beta) V_w^3 \tag{2}$$

Where ρ is the air density, and A is the swept area by the blades, V_w is the wind speed and C_p is the power coefficient of the wind speed, which can be expressed as [26]:

$$C_p(\lambda,\beta) = (0.44 - 0.0167\beta)\sin\frac{\pi(\lambda-3)}{15-0.3\beta} - 0.00184(\lambda-3)\beta \tag{3}$$

2.2 INDUCTION GENERATOR MODEL

Then, the self-excited IG dynamic model can be described as follows [27]:

$$\tfrac{d}{dt} i_{qs} = -R_s A_1 i_{qs} - \left(\frac{i_{qs} - i_{qLo} - i_{qL}}{C_o V_{ds}} + A_2\omega_m L_m\right) i_{ds} + R_r A_2 i_{qr} - A_1\omega_m L_r i_{dr} \tag{4}$$

$$\tfrac{d}{dt} i_{ds} = \left(\frac{i_{qs} - i_{qLo} - i_{qL}}{C_o V_{ds}} + A_2\omega_m L_m\right) i_{qs} - R_s A_1 i_{ds} + R_r A_2 i_{dr} + A_1\omega_m L_m i_{qr} - A_1 v_{ds} \tag{5}$$

$$\tfrac{d}{dt} i_{qr} = R_s A_2 i_{qs} + A_2\omega_m L_s i_{ds} - A_3 i_{qr} + \left(-\frac{i_{qs} - i_{qLo} - i_{qL}}{C_o V_{ds}} + A_1\omega_m L_s\right) i_{dr} \tag{6}$$

$$\tfrac{d}{dt} i_{dr} = -A_2\omega_m L_s i_{qs} + R_s A_2 i_{ds} + \left(\frac{i_{qs} - i_{qLo} - i_{qL}}{C_o V_{ds}} - A_1\omega_m L_s\right) i_{qr} - A_3 i_{dr} + A_2 v_{ds} \tag{7}$$

$$\tfrac{d}{dt}\omega_m = (-f\omega_m + PT_m + 1.5P^2 L_m (i_{qs} i_{dr} - i_{ds} i_{qr}))/J \tag{8}$$

$$\tfrac{d}{dt} v_{ds} = \frac{i_{ds} - i_{dLo} - i_{dL}}{C_o} \tag{9}$$

$$\tfrac{d}{dt} i_{qL} = \frac{1}{L}\left[-R\, i_{qL} - \left(\frac{i_{qs} - i_{qLo} - i_{qL}}{C_o\, v_{ds}}\right) L\, i_{dL}\right] \tag{10}$$

$$\tfrac{d}{dt} i_{dL} = \frac{1}{L}\left[v_{ds} - R\, i_{dL} + \left(\frac{i_{qs} - i_{qLo} - i_{qL}}{C_o\, v_{ds}} \right) L\;\; i_{qL} \right] \quad (11)$$

$$\tfrac{d}{dt} i_{qLo} = -\left(\frac{i_{qs} - i_{qLo} - i_{qL}}{C_o\, V_{ds}} \right) i_{dLo} \quad (12)$$

$$\tfrac{d}{dt} i_{dLo} = \frac{v_{ds}}{L_{eq}} + \left(\frac{i_{qs} - i_{qLo} - i_{qL}}{C_o\, V_{ds}} \right) i_{qLo} \quad (13)$$

All variables and symbols are defined at the nomenclature section.

SVC Model

It is simply a thyristor-controlled reactor shunted by a capacitor, shown in Fig. (2).

The equivalent reactance (X_{eq}) of the SVC is given by [28]:

$$X_{eq} = \frac{\pi \omega_s L}{2(\pi - \alpha) - \sin(2\alpha)} - \frac{1}{\omega_s c}$$

Where; (L, C) is the SVC inductance, and capacitance respectively.

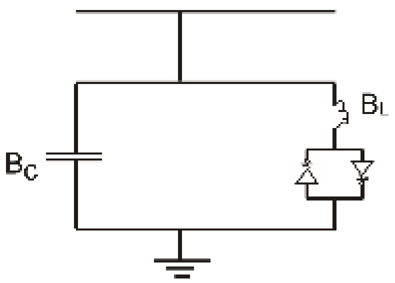

Figure : Simple SVC circuit.

SYSTEM CONTROLLERS

There are two paths of control are used here based on optimal pole shifting controller to regulate load voltage and frequency. The first path is dedicated for regulating the terminal voltage of the induction generator to a reference value via adjusting the firing angle of the thyristor of the SVAR. The second path is used to control the mechanical input power to the generator by adjusting the blade pitch angle of the wind turbine. A blade pitch actuator is used to control the mechanical power and hence the system rotational speed and consequently the terminal voltage frequency. The system controllers design and description are found in the next paragraphs.

Voltage Controller

The terminal voltage of the load can be controlled by adjusting the reactive power generated by the SVC. The SVC reactive power can be controlled by regulating the firing angel (α) of the back-to-back thyristors. The load voltage may be regulated according to an integration process as:

$$\tfrac{d}{dt} \alpha = k(V_r - v_d) \quad (14)$$

Where k, V_d , and V_r are constant, the actual voltage, and the reference load voltage respectively.

Frequency Controller

The load frequency is regulated by controlling the IG rotor speed. However, controlling the wind-turbine output power leads to controlling the IG rotor speed. So, controlling the blade angle (β) of the wind turbine leads to regulating the wind-turbine output power and hence the IG rotor speed according to the following equation:

$$\tfrac{d}{dt} \beta = k_1 (P_{ref} - P_t) \quad (15)$$

Where k_1, P_{ref}, and P_t are constant, the reference and actual values of wind turbine output power, respectively. The wind-turbine output power is a function in the wind turbine blade angle IG rotor speed, and wind velocity as seen in equation (2, 3).

The reference value of the wind-turbine output power is chosen in conditions of rated wind velocity, optimal tip-speed ratio of the wind turbine and zero wind-turbine blade angle.

OPTIMAL POLE SHIFTING CONTROL

In this study, the optimal pole shift algorithm presented in [29] has been applied. Where, this approach does not need the solution of non-linear algebraic Riccati equation. However, a linear Lyapunov for first order or second order equation is solved based on shifting one real or two complex conjugate poles, respectively. To shift the complex conjugate poles to a desired location only real part of the open-loop complex conjugate poles are shifted keeping the magnitude of imaginary parts preserved. An optimal feedback control law with respect to a quadratic performance index [29, 30] achieves the shift of real/complex conjugate poles. Consider a completely controllable linear time-invariant multivariable system represented as:

$$\dot{x}(t) = A_g x(t) + B_g u(t) \quad (16)$$

Where the dimensions of the state vector $x(t)$ and the control vector u are ($n \times 1$) and ($m \times 1$), respectively. A_g and B_g are constant plant matrices of appropriate dimensions. When a feedback control law $u = -K_{opt} x(t)$ is applied to (16), a closed-loop system is derived in the form:

$$\dot{x}(t) = A_c x(t) \quad (17)$$

where

$$A_c = A_g - B_g K_{opt} \tag{18}$$

Then, solving the following algebraic equation for a positive semi definite real symmetric solution P that satisfies Re(S_i) < 0 $\mathrm{Re}(\sigma_j) = \delta_j^2$ and $\sigma_j^2 = \delta_j^2$ with $j = 1,2,...,i$, where, σ_j and δ_j are the closed loop and open loop poles respectively with the feedback gain matrix $K_{opt} = B_g^T P$

$$PA_g + A_g^T P - PB_g B_g^T P = 0 \tag{19}$$

For any σ_j and δ_j which satisfy the optimality condition, the quantities

$\gamma_j = \frac{-(\mathrm{Re}(\sigma_j) + (\mathrm{Re}(\delta_j))}{2}$ In addition, $(\gamma_j + (\mathrm{Re}(\delta_j)$ are positive.

Let γ be a positive real constant scalar. Then for the following matrix algebraic equation:

$$P(A_g + \lambda I) + (A_g^T + \lambda I)P - PB_g R^{-1} B_g^T P = 0 \tag{20}$$

There exists a positive semi-definite real symmetric solution P satisfying: $\mathrm{Re}(\sigma_j) \le -\gamma$ and $(\sigma_j + \gamma)^2 = (\sigma_j + \gamma)^2$ with j = 1, 2, . . . , i and:

$$K_{opt} = R^{-1} B_g^T P \tag{21}$$

where R is a positive definite symmetric matrix for the given plant matrices (A_g, B_g). Also, the feedback control law $u = -K_{opt} x(t)$ minimizes the following quadratic performance index:

$$J = \int_0^\infty (x^T Q x + u^T R u) dt \tag{22}$$

With $Q = 2\gamma P$.

SIMULATION RESULTS

Digital simulations are obtained to validate the performance of the proposed optimal pole-shifting controller with the isolated WECS. The input to the proposed controller are the terminal voltage error and the generator's input power error. Moreover, the output of the controller are considered as TCR firing angle and the blade angle.

The entire system has been simulated on the digital computer using the Matlab / Simulink /software package. The specifications of the system used in the simulation procedure are listed in appendix [27]. The simulations have been carried out under load and wind velocity excursions.

The Ag, Bg and Cg matrices of the studied power system model are evaluated as:

$$A_g = \begin{bmatrix} -137.2 & -1940 & 81.8 & -2185 & 3.27 & 0.4 & 40.9 & 0 & 40.9 & 0 & 0 & -100 \\ 2233 & -96.3 & 2034 & 81.8 & 47 & -132.3 & -292.9 & 0 & -292.9 & 0 & 0 & 0 \\ 142.6 & 2034 & -87.9 & 2139 & -2.78 & -0.51 & -52.9 & 0 & -52.9 & 0 & 0 & 0 \\ -2037 & 89.6 & -2139 & -87.9 & -50.5 & 120.5 & 2.6 & 0 & 2.6 & 0 & 0 & 0 \\ -5.73 & 0.28 & -4.43 & 31.6 & -1.43 & 0 & 0 & 0 & 0 & 0 & 0 & -7.92 \\ 0 & 4734 & 0 & 0 & 0 & 0 & 0 & -4734 & 0 & -4734 & 0 & 0 \\ -36.1 & 0 & 0 & 0 & 0 & 0.35 & 36.1 & -46.15 & 36.1 & 0 & 0 & 0 \\ 240 & 0 & 0 & 0 & 0 & -2.3 & -194.6 & -2.1 & -240.7 & 0 & 0 & 0 \\ -4 & 0 & 0 & 0 & 0 & 0.04 & 4 & 0 & 4 & -46.15 & 0 & 0 \\ 6 & 0 & 0 & 0 & 0 & 15.2 & -6 & 0 & 40.1 & 0 & -295.6 & 0 \\ 0 & -100 & 0 & 0 & 0 & 0 & 0 & 0 & 0 & 0 & 0 & 0 \\ 0 & 0 & 0 & 0 & 0.85 & 0 & 0 & 0 & 0 & 0 & 0 & 22.23 \end{bmatrix}$$

$$B_g = \begin{bmatrix} 0 & 0 & 0 & 0 & 0 & 0 & 0 & 0 & 0 & 0 & 1 & 0 \\ 0 & 0 & 0 & 0 & 0 & 0 & 0 & 0 & 0 & 0 & 0 & 1 \end{bmatrix}'$$

$$C_g = \begin{bmatrix} 0 & 0 & 0 & 0 & 0 & 1 & 0 & 0 & 0 & 0 & 0 & 0 \\ 0 & 0 & 0 & 0.85 & 0 & 0 & 0 & 0 & 0 & 0 & 0 & 22.23 \end{bmatrix}$$

The performance of the proposed scheme has been tested with a turbulence change in wind speed. In addition, the system response is investigated during a step change of load impedance.

Simulation results depicting the variation of different variables with step turbulence in wind speed are shown in Fig. (3). The wind speed is assumed to vary between 8.5 m/s and 11.5 m/s. It has been noticed that as the wind velocity increases, the firing angle of the thyristor will decrease. This is because, at higher wind speed, the shaft torque output of the wind turbine increases and tends to increase the rotor speed of the induction generator. The control action can be summarized as follows:

a) If the terminal voltage tends to increase due to the increase in wind speed, the controller comes into operation and decreases the firing angle of the thyristor. This would result in reducing the equivalent inductance of the reactor in the SVAR and, in turn, increasing the reactor current. Consequently, the total effective load on the induction generator will increase. The terminal voltage tends to reduce and settles down to the reference value.

b) If the electrical frequency of the generator tends to increase due to the increase in wind speed, the controller will increase the blade angle causing the mechanical input power to decrease. This will reduce the rotor speed and so the terminal frequency.

c) If the terminal voltage and /or frequency tries to decrease due to reduced wind velocity, the controller will take an action, which is opposite to that outlined above.

Figure (4) shows simulation results of the proposed system with step change in load impedance. It is seen that the action of the controller, with a step increase in load impedance (or a decrease in load current) is similar to that with an increase in wind velocity and vice versa. Thus, if the load impedance is assumed to be abruptly increased, the load current will decrease. In response to the load reduction, the terminal voltage tend to rise. Therefore, the proposed controller comes into action and decreases the firing angle of the thyristor. This is, in turn, will increase the reactor current causing the effective load on the induction generator to increase, and in turn, the terminal voltage to restore its reference. In addition, reduction in load current leads to increase in rotor speed and hence in the electrical frequency of the generator, so the controller will increase the blade angle causing the mechanical input power to decrease. This will reduce the rotor speed and so the terminal frequency.

On the other hand, if the load impedance decreases, the controller increases the thyristor firing angle, which decreases the reactor current and decreases the blade angle to compensate for the load increase.

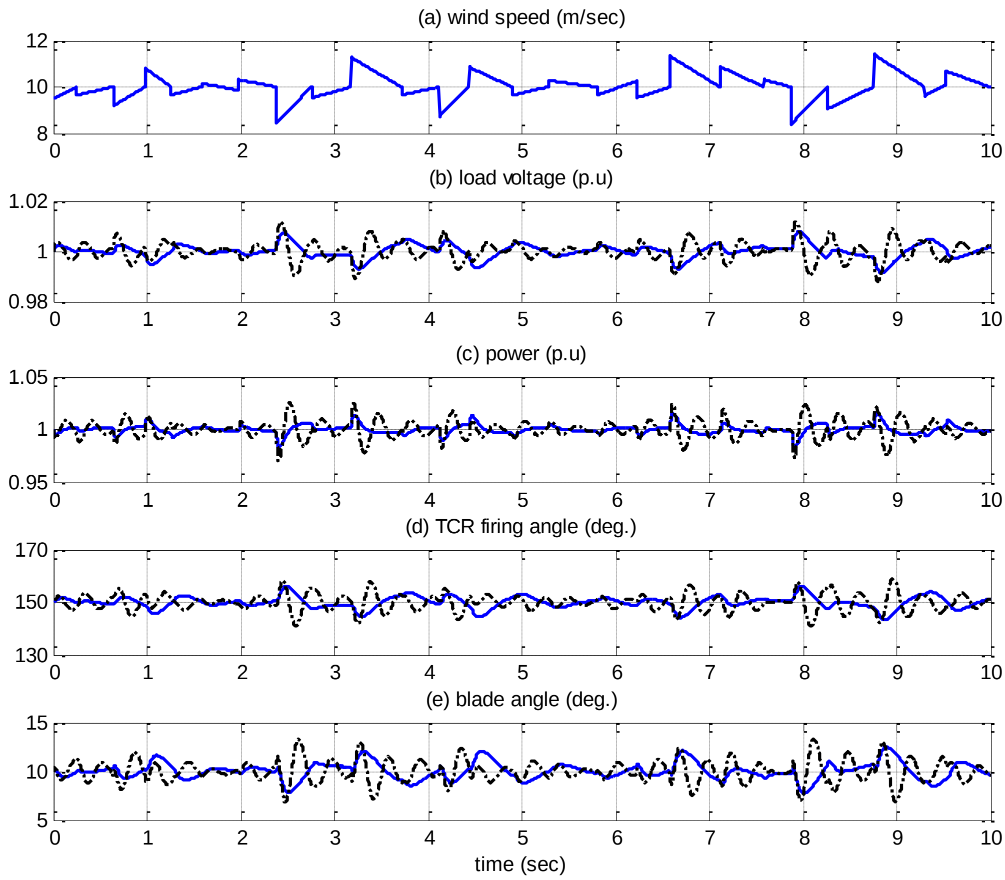

International Journal of Applied Engineering Research ISSN 0973-4562 Volume 12, Number 17 (2017) pp. 6720-6729

Figure 3: Simulation results of the proposed scheme with step change in wind speed

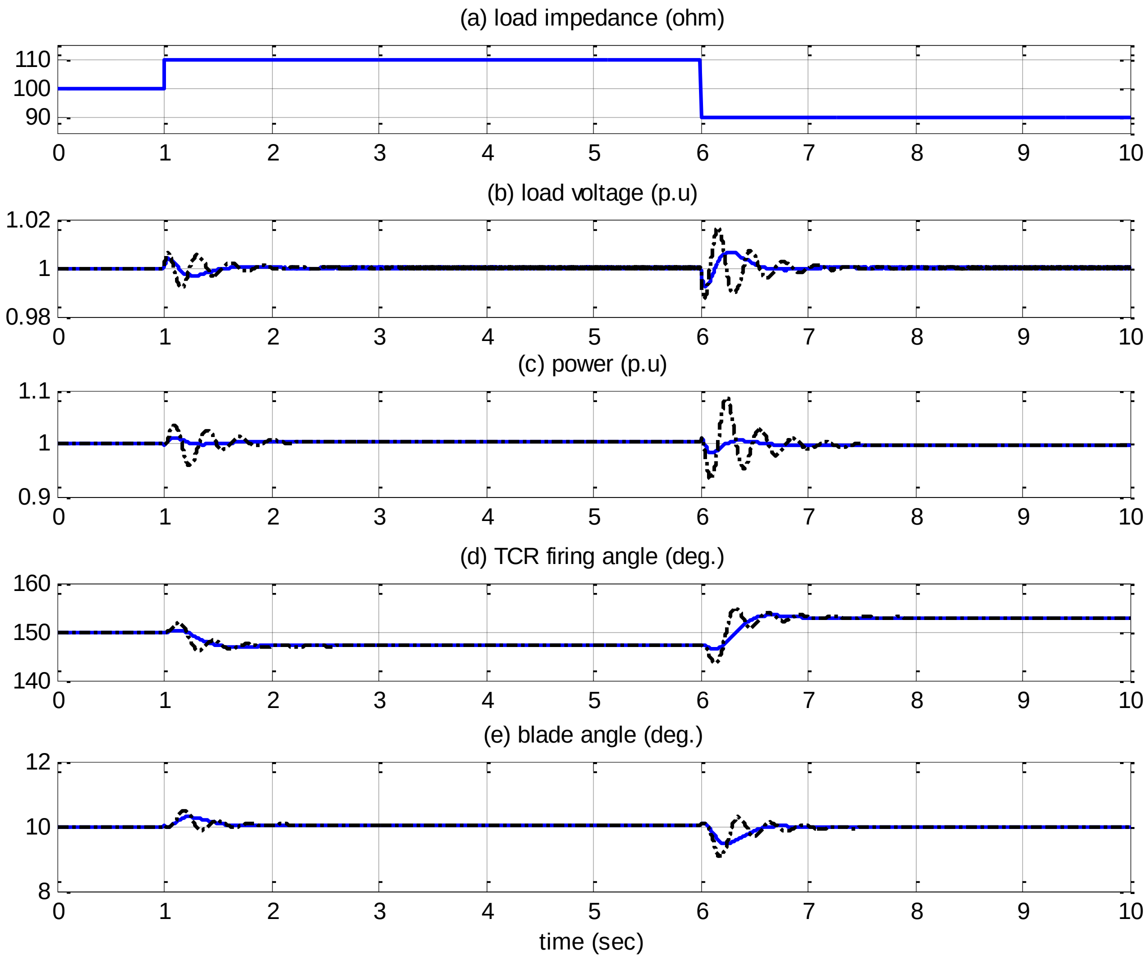

Figure 4: Simulation results of the proposed scheme with step change in load impedance.

Robustness

Since our concerns are also in robust stability against various model uncertainties, some system parameters have been changed as follows:

i) The stator and rotor resistances are assumed to increase by 20% above nominal values.

ii) The moment of inertia is assumed to rise 20% above nominal.

iii) The magnetizing inductance is assumed to be 10% less than nominal.

For perturbed system the responses are shown in Fig. (5) and Fig. (6). It should be seen that the system is robustly stable in spite of parameters variations.

It has been indicated in the figures that the controller is able to stabilize the terminal voltage and frequency with high accuracy in spite of modeling errors.

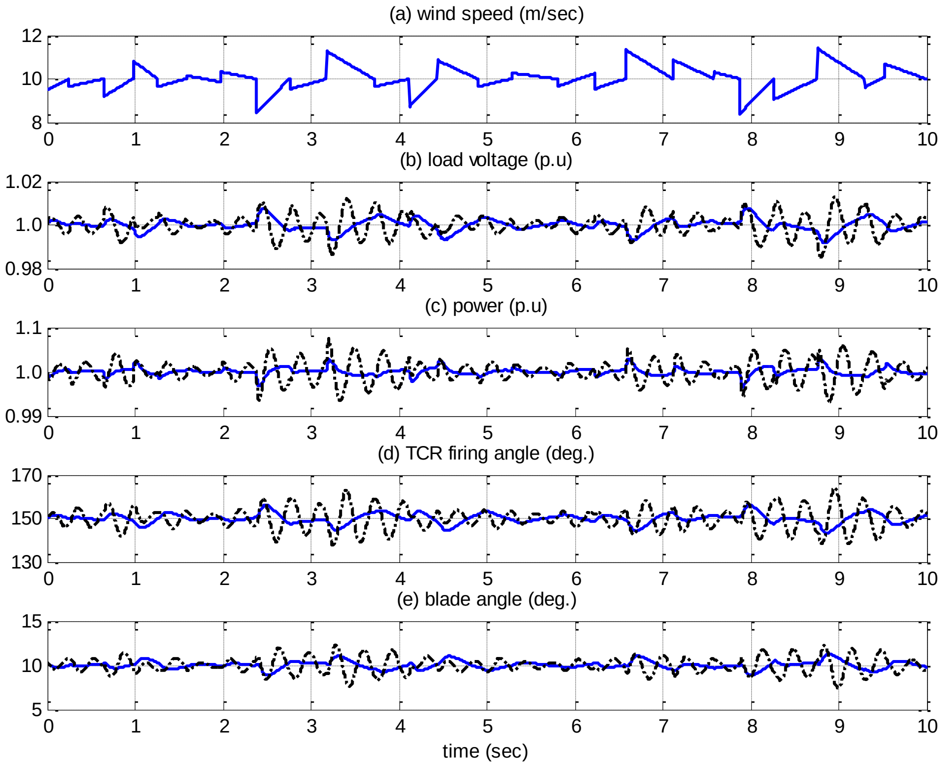

Figure 5: Simulation results of the proposed scheme with step change in wind speed with parameters change.

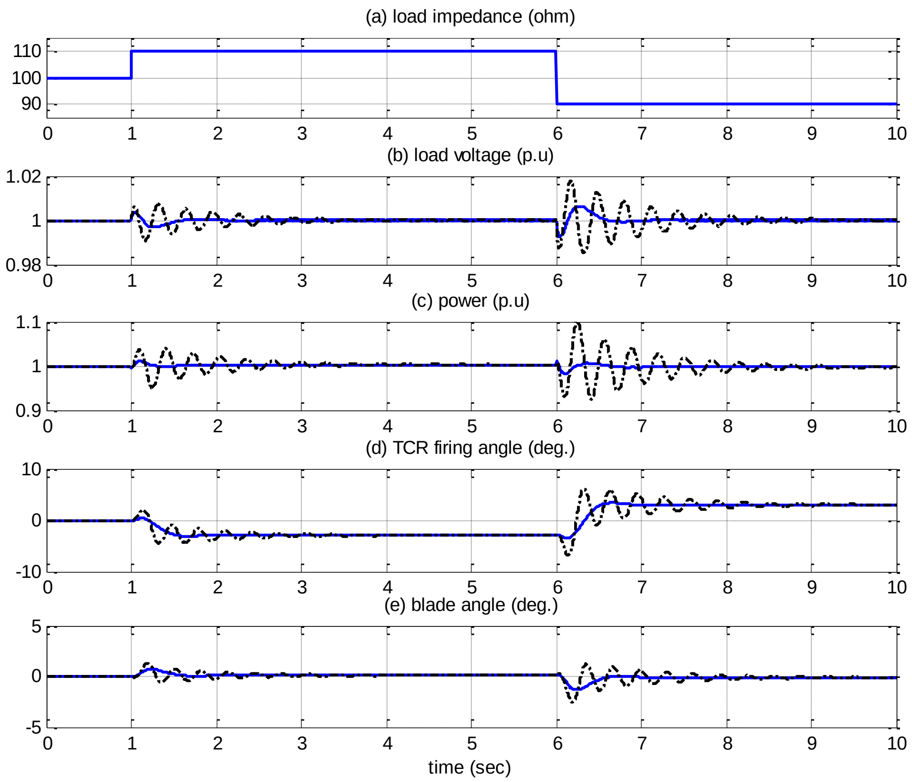

Figure 6: Simulation results of the proposed scheme with step change in load impedance with parameters change.

CONCLUSIONS

This paper investigates the robust optimal pole-shifting controller to control the terminal voltage and frequency of a SEIG. The SEIG driven by wind turbine and feeding static load. This scheme consists of a wind turbine, induction generator, SVAR compensator (fixed capacitor in parallel with thyristor controlled reactor), and static load. The firing angle of the thyristor is controlled according to the error between the reference and actual load voltages. Also, the rotor speed is adjusted by controlling the blade pitch-angle according to the error between the reference and actual mechanical power input to the generator. The complete nonlinear dynamic model of the system has been described and linearized around an operating point.

Digital simulations have been carried out in order to evaluate the effectiveness of the proposed scheme. The wind energy system with the proposed controller has been tested through turbulence changes in wind speed and step changes in load impedance. The results prove that the proposed controller is successful in regulating the terminal voltage and frequency of a stand-alone wind energy conversion system under wind and/or load excursion and it is robust against system parameters change.

NOMENCLATURE

v_{ds}, v_{qs} d-q stator voltages,

i_{ds}, i_{qs} d-q stator currents,

i_{dr}, i_{qr} d-q rotor currents,

R_s, R_r stator and rotor resistances per phase,

L_s, L_r, L_m Stator, rotor, and magnetizing inductances

C_0 Self excitation capacitance per phase,

ω_s Angular stator frequency of the induction generator,

ω_m Angular rotor speed (electrical rads/sec) of the induction generator,

ω_t Angular rotor speed of the turbine,

J Moment of inertia,

f Friction coefficient,

L_o Physical inductance of the reactor in the SVAR,

α Firing angle of the SVAR,

β Turbine blade pitch angle,

i_{dL}, i_{qL} d-q load current,

i_{dLo}, i_{qLo} d-q reactor current in the SVAR,

λ Turbine tip speed-ratio,

P Number of pole pairs.

REFERENCES

[1] Mendis, N., Muttaqi, K. M., Sayeef, S., and Perera, S.: 'Standalone operation of wind turbine-based variable speed generators with maximum power extraction capability', IEEE Trans. on Energy Conv., 2012, 27, (4), pp 822-834.

[2] Monmasson, E., Idkhajine, L., Cirstea, M. N., Bahri, I., Tisan, A., and Naouar, M. W.: 'FPGAs in industrial control applications', IEEE Trans. Ind. Informat., 2011, 7, (2), pp 224–243.

[3] Teodorescu, R., Lissere, M., and Rodriguez, P.: 'Grid Converter for Photovoltaic and Wind Power Systems' (Wiley Press, 2011, 1st edn.).

[4] Yang, L. S, and Liang, T. J.: 'Analysis and implementation of a novel bidirectional DC–DC converter', IEEE Trans. Ind. Electron., 2012, 59, (1), pp 422–434.

[5] Wind Energy Systems by Dr. Gary L. Johnson, 2001.

[6] J. M. Carrasco *et al*., "Power-Electronic Systems for the Grid Integration of Renewable Energy Sources: A Survey," in *IEEE Transactions on Industrial Electronics*, vol. 53, no. 4, pp. 1002-1016, June 2006. doi: 10.1109/TIE.2006.878356

[7] Anaya-Lara O., Jenkins N., Ekanayake J., Cartwright P., Hughes M. Wind Energy Generation Modelling and Control. 1st edition, Chichester: John Wiley & Sons Ltd. 2009.

[8] J. Sallan, E. Muljadi, M. Sanz and C. P. Butterfield "Control of self-excited induction generators driven by wind turbines" IEEE Trans. on Energy Conversion, Vol. 12, 2000.

[9] T.F. Chan and Loi Lei Lai "steady-state analysis and performance of a stand-alone three-phase induction generator with asymmetrically connected load impedances and excitation capacitances". IEEE Trans. On Energy Conversion, Vol. 16, No. 4, Dec. 2001, pp 91-96.

[10] E. Muljadi, J. Sallan, M. Sanz and C. P. Butterfield "Investigation of self-excited induction generators for wind turbine applications" IEEE Trans. on Energy Conversion, Vol. 12, 2000

[11] Kassa Idjdarene, Djamila Rekioua, Toufik Rekioua, and

Abdelmouna¨ım Tounzi, "performance of an isolated induction generator under unbalanced loads". IEEE TRANSACTIONS ON ENERGY CONVERSION, VOL. 25, NO. 2, JUNE 2010, pp 303-311.

[12] S. C. Kuo and L. Wang “Analysis of voltage control for a self-excited induction generator using a current-controlled voltage source inverter (CC-VSI)” IEE Proc. Gener. Transm. Distrib., Vol. 148, No. 5, p 431-437, September 2001.

[13] D. Seyoum, M. Rahman, and C. Grantham," Terminal voltage control of a wind turbine driven isolated induction generator using stator oriented field control", Proc. Of the IEEE Eighteenth Annual Applied Power Electronics Conference and Exposition, Vol. 2, Feb. 2003, pp 846-852.

[14] B.A.Zahir, J. G. Kettleborough and I. R. Smith, "a stand alone induction generator model producing a constant voltage constant frequency output". IEEE 4th International Conference on Emerging Technologies, Vol. 1, 2008, pp 83-86.

[15] D.G. Forchetti, J.A. Solsona, G.O. Garc and M.I. Valla, "A control strategy for stand-alone wound rotor induction machine". Electric Power Systems Research, Vol. 77, pp 163–169, 2007.

[16] Lotfi Krichen, Bruno Francois and Abderrazak Ouali, "A fuzzy logic supervisor for active and reactive power control of a fixed speed wind energy conversion system". Electric Power Systems Research, Vol. 78, pp 418–424, 2008.

[17] Yang, X., and Wu, X. L.: 'Integral fuzzy sliding mode control for variable speed wind power system', Proc. IEEE Int. Conf. on Automation and Logistics, Jinan, China, pp1289-1294, August 2007.

[18] Zhang, X., Wang, W., and Liu, Y.: 'Fuzzy control of variable speed wind turbine', in Proc. 6th World Congress on Intelligent Control and Automation, Dalian, China, pp 3872-3876, 2006.

[19] Prats, M., Carrasco, J., Galvan, E., Sanchez, J., Franquelo, L., and Batista, C.: 'Improving transition between power optimization and power limitation of variable speed, variable pitch wind turbines using fuzzy control techniques', Proc. IECON, Nagoya, Japan, pp1497-1502, October 2000.

[20] A. Abdin and X. Wilson, "Control design and dynamic performance analysis of a wind turbine-induction generator unit", IEEE Trans. On Energy Conversion, Vol. 15, No. 1, March 2000, pp 91-96.

[21] Ahmed M. Kassem, "Advanced control techniques for regulating the voltage and frequency of a wind driven induction generator". PhD thesis, Assuit University, 2006.

[22] GEl-SHERBINY, M. K.—HASAN, M. M.—El-SAADY, G.— YOUSEF, A. M. : Optimal pole shifting for power system stabilization., Electric Power Syst. Research No. 66 (2003), 253–258.

[23] KISHOR, N.—SAINI, R. P.—SINGH, S. P. : Coordinated control for the exciter and governor in a small hydropower plant, Proc. of National Power System Conference, Indian Institute of Technology, Madras, Dec. 27–30, 2004, 431–436.

[24] S. J. P. S. Mariano, J. A. N. Pombo, M. R. A. Calado and L. A. F. M. Ferreira, "Pole-shifting procedure to specify the weighting matrices for a load-frequency controller," *Melecon 2010 - 2010 15th IEEE Mediterranean Electrotechnical Conference*, Valletta, 2010, pp. 818-823. doi: 10.1109/MELCON.2010.5475958

[25] N. Kishor, "Oscillation Damping With Optimal Pole-Shift Approach in Application to a Hydro Plant Connected as SMIB System," in *IEEE Systems Journal*, vol. 3, no. 3, pp. 317-330, Sept. 2009. doi: 10.1109/JSYST.2009.2022577

[26] A. M. Kassem and S. A. Zaid, "Load parameter waveforms improvement of a stand-alone wind-based energy storage system and Takagi–Sugeno fuzzy logic algorithm," in *IET Renewable Power Generation*, vol. 8, no. 7, pp. 775-785, September 2014. doi: 10.1049/iet-rpg.2013.0382

[27] A. A. Hassan, Yehia S. Mohamed and Ahmed M. Kassem, " Voltage and Frequency Control of An Isolated Wind Driven Induction Generator Based On H∞ Approach", The 4th Saudi Tech. Conf. and Exhib., (STCEX06), Dec. 2006.

[28] Rashid, M.: 'Power Electronics Handbook' (Elsevier Press, 2011, 2nd edn.)

[29] Nand Kishor, R. P. Saini, S. P. Singh, "optimal pole shift control in application to a hydro power plant". Journal of electrical engineering, VOL. 56, NO. 11-12, 2005, pp. 290–297

[30] M.H. Amin, "Optimal pole shifting for continuous multivariable linear systems", Int. J. Control, vol. 41, no. 3, pp.701-707, 1985.

APPENDIX:

System parameters

Wind turbine:

Rating : 1 kw , 450 rpm (low speed side) at $V_w = 12$ m/s .

Size : Height = 4 m, Equator radius = 1 m, Swept area = 4 m^2, ρ = 1.25 kg/ m^2.

Induction machine:

Rating : 3-phase , 2 kw , 120 V , 10 A , 4-pole , 1740 rpm .

Parameters: $R_s = 0.62\Omega$, $R_r = 0.566\Omega$, $L_s = L_r = 0.058174$ H., $L_m = 0.054$ H, $J = 0.0622$ kg.m^2, $f = 0.00366$ N.m./rad/s.

FC-TCR : C_o = 176 μF, L_o = 0.127